

ALMA MATER STUDIORUM · UNIVERSITÀ DI BOLOGNA

Scuola di Scienze
Dipartimento di Fisica e Astronomia
Corso di Laurea in Fisica

Comparison of radiobiological effects induced by ultra-high and standard dose rate of x-rays on a radio-resistant cell line

Relatore:
Prof. Gastone Castellani

Presentata da:
Maria Stefania Petrigliano

Correlatore:
Dott.ssa Isabella Zironi

Anno Accademico 2015/2016

INDEX

ABSTRACT

BACKGROUND

1. IONIZING RADIATION	3
1.1.1. INTERACTION PHOTONS WITH MATTER	4
1.1.2. INTERACTION ELECTRON WITH MATTER.....	6
1.1.3. QUANTITY TO DESCRIBE INTERACTIONS	6
1.1.4. DOSIMETRIC QUANTITIES AND UNITS.....	8
2. IRRADIATION OF CELLS.....	10
2.1. THE CELL	10
2.2. WATER RADIOLYSIS AND GENERATION OF REACTIVE OXYGEN SPECIES	12
2.3. FUNDAMENTALS OF IONIZING RADIATION BIOCHEMISTRY	13
2.4. IR-INDUCED CELL DEATH OUTCOMES	15
3. X RAY IN RADIOTHERAPY.....	18
3.1. X-RAY TUBE	18
3.1.1. RAY TUBE X BALTEAU CSC320 / 70	19
3.2. PLASMA FOCUS	19
3.2.1. PFMA-3	20
3.3. DOSE RATE	21

MATERIALS AND METHODS

1. CELLS AND CELL CULTURE.....	23
2. IRRADIATION	23
2.1.1. IRRADIATION WITH PF	24
2.1.2. IRRADIATION WITH RAY TUBE X BALTEAU CSC320/70.....	24
3. ADHESION AND PROLIFERATION ASSAY	24
4. MIGRATION ASSAY	25

RESULTS

CONCLUSIONS

ABSTRACT

Radiotherapy (RT) has recently evolved with the emergence of heavy ion radiations or new fractionation schemes of photon therapy, which modify the dose rate of treatment delivery. The aim of the present study was then to evaluate the *in vitro* influence of a ultra-high dose rate comparing them with standard dose rate.

In this regard, a radioresistant SK-MEL-28 cell line were irradiated with x-ray in order to have a total dose of 2 and 4 Gy, at two different dose rate. The ultra-high dose rate is a specific property of the dense plasma focus (DPF) device, which has pulsed operation and thus gives short and highly energetic pulses of multiple types of rays and particles, in this case, we focused our study on the influence of X-rays. While a low dose rate is obtained with conventional X-ray tube.

In this study it results that a ultra-high dose rate enhances radiosensitivity of melanoma cells while reducing the adhesion, proliferation and migration ability of cells.

Riassunto

La radioterapia (RT) si è recentemente sviluppata con l'emergere delle radiazioni prodotte da ioni pesanti o con i nuovi schemi di frazionamento utilizzati in fototerapia, i quali modificano il dose rate del trattamento somministrato. Lo scopo del presente studio è stato quindi quello di valutare l'influenza *in vitro* di un ultra-high dose rate confrontandoli con uno standard dose rate.

A questo proposito, la radioresistente linea cellulare SK-MEL-28 è stata irradiata con raggi x per avere una dose totale di 2 e 4 Gy, con i due differenti dose rate. L'ultra-high dose rate è una specifica proprietà del dispositivo Plasma focus (DPF), che lavora ad impulsi e fornisce quindi brevi impulsi e altamente energetici di diversi tipi di raggi e particelle, in questo caso, abbiamo concentrato il nostro studio sull' influenza dei raggi-X. Mentre un basso dose rate è ottenuto con tubo a raggi X convenzionale.

In questo studio risulta che l'ultra-high dose rate migliora radiosensibilità delle cellule di melanoma riducendo la capacità delle cellule di aderire, proliferare e migrare.

BACKGROUND

1. IONIZING RADIATION

In physics, radiation is the emission or transmission of energy in the form of waves or particles through space or through a material medium. Radiation is often categorized as either ionizing or non-ionizing depending on the energy of the radiated particles.

Ionizing radiation is electromagnetic wave and particles with sufficiently high energy to remove electrons in matter, that is able to ionize the atoms or molecules. The minimum energy that must have radiation is 10 eV, as is binding energy of more external electron of atoms.

The ionizing radiation can be divided in two groups:

- **Indirectly ionizing:**

To indirectly ionizing radiation means neutral particles that supply all or part of their energy to directly ionizing particles. In this sense the energy transfer to the medium asks an intermediate step, for which such radiation is not able to ionize the medium in a direct manner. Fall into this category the neutrons, γ ray and x ray.

- **Directly ionizing**

Any charged massive particle can ionize atoms directly by fundamental interaction through the Coulomb force if it carries sufficient kinetic energy. This include electrons, protons and other charge particles.

The mechanisms by which ionizing radiation directly interact with matter at the atomic level are the excitation and ionization.

In the excitations, the energy transferred is less than that required to expel from the atom one of its outer orbital electrons (valence electrons), whose binding energy is of the order of 10 eV. Because of the interaction of these low-energy radiation, the atom goes from the ground state to an excited state for the orbital movement of one or more electrons, still within the same atom.

In the ionization energy imparted by radiation exceeds that of the electron valence bond that is then ejected from the membership. Following this event creates a pair of ions: on the one hand the electron, or negative ion, and the other, the atom, that losing the electron and become a positive ion. A very important feature of ionizing radiation, and in particular of hadrons, is their typical curve of

ionization; this curve leads to the release of a relatively low dose of energy along the entire route of the hadrons, except for a significantly reduced region, where there is the "ionization Bragg peak", in which they stop releasing all their energy.

1.1.1. INTERACTION PHOTONS WITH MATTER

In general, the indirectly ionizing radiation produced by photons interacting in the following ways:

- **Reyleigh diffution**

In coherent (Rayleigh) scattering the photon interacts with a bound orbital electron (i.e. with the combined action of the whole atom). The event is elastic in the sense that the photon loses essentially none of its energy and is scattered through only a small angle. Since no energy transfer occurs from the photon to charged particles, Rayleigh scattering plays no role in the energy transfer coefficient; however, it contributes to the attenuation coefficient.

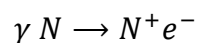
In tissue and tissue equivalent materials the relative importance of Rayleigh scattering in comparison with other photon interactions is small, as it contributes only a few per cent or less to the total attenuation coefficient.

- **Photoelectric effect**

the photoelectric effects are normally predominates in the interaction of photons with matter at low energy. In the process a photon is completely absorbed by an internal electron atom (the effect is predominant with longer bound electrons, i.e. those closest to the nucleus) which is ejected with energy equal to that of the photon less its binding energy

$$E_{e^-} = h\nu - E_b$$

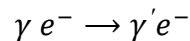
This effect results from the interaction of the photon with the whole atom rather than with the single electron. the core absorbs part of the photon pulse according to the reaction



- **Compton effect**

The Compton effect is the process of diffusion of a photon of an atomic electron and is more likely to occur with electrons of the outermost orbitals. The outer electrons, due to the small bond energy, can be well approximated as free.

In the interaction the photon is not absorbed, but is broadcast with a lower energy than that of incidence according to the reaction



The change in photon wavelength $\Delta\lambda$ is given by the well known Compton relationship:

$$\Delta\lambda = \lambda_c(1 - \cos\theta)$$

where $\lambda_c = h / m_e c = 0.024 \text{ \AA}$ is the Compton wavelength of electron.

- **Pair production**

In pair production the photon disappears and an electron–positron pair with a combined kinetic energy equal to $h\nu - 2m_e c^2$ is produced in the nuclear Coulomb field.

Since mass is produced out of photon energy in the form of an electron–positron pair, pair production has an energy threshold (minimum photon energy required for the effect to happen) of $2m_e c^2 = 1.02 \text{ MeV}$. In our case we are at lower energies therefore does not occur.

- **Effects following photon interactions**

In the photoelectric effect, the Compton effect and triplet production, vacancies are produced in atomic shells through the ejection of orbital electrons. For the orthovoltage and megavoltage photons used in the diagnosis and treatment of disease with radiation, the shell vacancies occur mainly in inner atomic shells and are followed by characteristic X rays or Auger electrons, the probability for the former given by the fluorescent yield w , while the probability for the Auger effect is $1 - w$. Pair production and triplet production are followed by the annihilation of the positron with a ‘free’ and stationary electron, producing two annihilation quanta, most commonly with energies of 0.511 MeV each and emitted at 180° from each other to satisfy the conservation of charge, momentum and energy. An annihilation of a positron before it has expended all of its kinetic energy is referred to as annihilation in flight and produces photons with energies exceeding 0.511 MeV

1.1.2. INTERACTION ELECTRON WITH MATTER

The electrons interacting with matter may lose energy in two ways:

- **Electron–orbital.** Electron interactions Coulomb interactions between the incident electron and orbital electrons of an absorber result in ionizations and excitations of absorber atoms:
 - ✓ Ionization: ejection of an orbital electron from the absorber atom;
 - ✓ Excitation: transfer of an orbital electron of the absorber atom from an allowed orbit to a higher allowed orbit (shell).

Atomic excitations and ionizations result in collisional energy losses and are characterized by **collision (ionization) stopping powers**.

- **Electron–nucleus interactions.** Coulomb interactions between the incident electron and nuclei of the absorber atom result in electron scattering and energy loss of the electron through production of X ray photons (bremsstrahlung). These types of energy loss are characterized by **radiative stopping powers**.

The total mass coefficient:

$$(\mathbf{S}/\rho)_{\text{tot}} = (\mathbf{S}/\rho)_{\text{c}} + (\mathbf{S}/\rho)_{\text{r}}$$

Is the sum of two coefficients batches (collision and radiation).

1.1.3. QUANTITY TO DESCRIBE INTERACTIONS

- **Cross section**

The collision and interaction between ionizing radiation and matter is described in terms of cross section, defined as the probability that a given reaction or a physical process can happen. Physically the cross section represents the probability with which the electromagnetic radiation interacts with a given target, be it a homogeneous medium or a single atom.

$$\frac{\Delta N}{N} = -\sigma N_a \Delta x$$

Were: Δx is the thickness of target; N_a is the number of atom per cm^3 of target ; N is the number of particles sent on a cm^2 of target in 1s.

This probability is a function of energy, the type of radiation and the target material.

- **Coefficient of linear attenuation**

Thanks to the cross section, for indirectly ionizing radiation, we can determine another quantity called coefficient of linear attenuation

$$\mu = \rho \frac{N_A}{A} \sigma = N_b \sigma$$

The cross section and linear attenuation coefficient introduced so far are characteristic quantities of the medium, and are the true indicators of the interaction between radiation and matter.

- **LET**

For a complete understanding of ionizing radiation on living material it is of fundamental importance to know the spatial distribution of energy transferred along the tracks of charged particles, that is the ionization capacity specification. This is defined by the 'Linear Energy Transfer (LET)'. In mathematical terms is defined by:

$$L_{\Delta} = \left(\frac{dE}{dx} \right)_{\Delta}$$

where dE is the energy loss of the charged particle due to electronic collisions while traversing a distance dx , excluding all secondary electrons with kinetic energies larger than Δ . (If Δ tends toward infinity, then there are no electrons with larger energy, and the linear energy transfer becomes the unrestricted linear energy transfer which is identical to the linear electronic stopping power)

X rays and γ rays are considered low LET (sparsely ionizing) radiations, while energetic neutrons, protons and heavy charged particles are high LET (densely ionizing) radiations.

1.1.4. DOSIMETRIC QUANTITIES AND UNITS

Since the energy lost by the radiation during the interaction does not necessarily coincide with the energy absorbed by the medium, the transfer processes and energy absorption are distinguished as two multistage process of the interaction of radiation with matter, have thus introduced the magnitudes called dosimetric quantities. The most commonly used dosimetric quantities and their units are defined below.

- **KERMA**

Kerma is an acronym for ‘kinetic energy released per unit mass’. It is a non stochastic quantity applicable to indirectly ionizing radiations such as photons and neutrons. It quantifies the average amount of energy transferred from indirectly ionizing radiation to directly ionizing radiation without concern as to what happens after this transfer. In the discussion that follows we will limit ourselves to photons. The energy of photons is imparted to matter in a two stage process. In the first stage, the photon radiation transfers energy to the secondary charged particles (electrons) through various photon interactions (the photoelectric effect, the Compton effect, pair production, etc.). In the second stage, the charged particle transfers energy to the medium through atomic excitations and ionizations. In this context, the kerma is defined as the mean energy transferred from the indirectly ionizing radiation to charged particles (electrons) in the medium per unit mass dm :

$$K = \frac{d\bar{E}_{tr}}{dm}$$

The unit of kerma is joule per kilogram (J/kg). The name for the unit of kerma is the gray (Gy), where $1 \text{ Gy} = 1 \text{ J/kg}$.

- **Absorbed dose**

Absorbed dose is a non-stochastic quantity applicable to both indirectly and directly ionizing radiations. As mentioned before, in the first step (resulting in kerma), the indirectly ionizing radiation transfers energy as kinetic energy to secondary charged particles. In the second step, these charged particles transfer some of their kinetic energy to the medium (resulting in absorbed dose) and lose some of their energy in the form of radiative losses (bremsstrahlung, annihilation in flight).

The absorbed dose is related to the stochastic quantity energy imparted. The absorbed dose is defined as the mean energy \bar{E}_{ass} imparted by ionizing radiation to matter of mass m in a finite volume V by:

$$D = \frac{d\bar{E}_{ass}}{dm}$$

The energy imparted \bar{E}_{ass} is the sum of all the energy entering the volume of interest minus all the energy leaving the volume, taking into account any mass– energy conversion within the volume. The unit is the gray (Gy).

2. IRRADIATION OF CELLS

When ionizing radiation is absorbed in biological material, the damage to the cell may occur in one of two ways:

- **Direct action in cell damage by radiation.**

In direct action the radiation interacts directly with the critical target (nucleic acids, proteins, lipids etc.) in the cell. The atoms of the target itself may be ionized or excited through Coulomb interactions, leading to the chain of physical and chemical events that eventually produce the biological damage. Direct action is the dominant process in the interaction of high LET particles with biological material.

- **Indirect action in cell damage by radiation**

In indirect action the radiation energy may cause radiolysis of intracellular water molecules leading to production of ROS and free radicals, which can, through diffusion in the cell, damage the critical target within the cell, in particular on the fat constituting the membranes (liperoxidation processes), on sugars and phosphates, on the nucleus protein and on the DNA where alter the genetic information. About two thirds of the biological damage by low LET radiations (sparsely ionizing radiations) such as X rays or electrons is due to indirect action.

2.1. THE CELL

The cell (from Latin cella, meaning "small room") is the basic structural, functional, and biological unit of all known living organisms. A cell is the smallest unit of life that can replicate independently, and cells are often called the "building blocks of life".

There are two types of cells, eukaryotic and prokaryotic. Eukaryotic cells contain membrane-bound organelles, such as the nucleus, while prokaryotic cells do not. Differences in cellular structure of prokaryotes and eukaryotes include the presence of mitochondria and chloroplasts, the cell wall, and the structure of chromosomal DNA.

Moving from the inside to the outside of the eukaryotic cell, we find the **nucleus** surrounded by nuclear envelope (double membrane) perforated by nuclear pores, which regulate entry and exit of materials. Within the nucleus, the DNA is organized into discrete units called chromosomes, structures that carry the genetic information. Each chromosome contains one long DNA molecule

associated with many proteins. nucleus. The complex of DNA and proteins making up chromosomes is called chromatin.

Within the eukaryotic cell, in addition to the nucleus, there are organelles of different type are also separated from the environment by means of specific intracellular membranes. These membranes are part of a system called the **endomembrane system**, which includes the nuclear envelope, the endoplasmic reticulum, the Golgi apparatus, lysosomes, various kinds of vesicles and vacuoles, and plasma membrane. This system carries out a variety of tasks in the cell, including synthesis of proteins, transport of proteins into membranes and organelles or out of the cell, metabolism and movement of lipids, and detoxication of poisons.

Continuing our tour of the cell we find some organelles that are not closely related to the endomembrane system but play crucial roles in the energy transformations carried out by cells: **Mitochondria** (singular, mitochondrion) are the sites of cellular respiration, the metabolic process that uses oxygen to generate ATP by extracting energy from sugars, fats, and other fuels. **Chloroplasts**, found in plants and algae, are the sites of photosynthesis. These organelles convert solar energy to chemical energy by absorbing sunlight and using it to drive the synthesis of organic compounds such as sugars from carbon dioxide and water.

The membrane-enclosed organelles constitute one level of the organizational substructure of eukaryotic cells. A further level of organization is provided by the **cytoskeleton**, which consists of a network of protein filaments extending throughout the cytoplasm of all eukaryotic cells. The cytoskeleton is composed of three principal types of protein filaments: actin filaments, intermediate filaments, and microtubules, which are held together and linked to subcellular organelles and the plasma membrane by a variety of accessory proteins. The cytoskeleton provides a structural framework for the cell, serving as a scaffold that determines cell shape and the general organization of the cytoplasm. In addition to playing this structural role, the cytoskeleton is responsible for cell movements. These include not only the movements of entire cells, but also the internal transport of organelles and other structures (such as mitotic chromosomes) through the cytoplasm. Importantly, the cytoskeleton is much less rigid and permanent than its name implies. Rather, it is a dynamic structure that is continually reorganized as cells move and change shape, for example, during cell division.

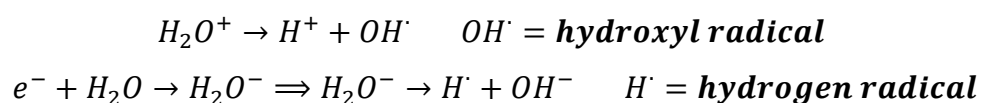
Finally the cell is surrounded by a **plasma membrane**, which defines the boundary of the cell and separates its internal contents from the environment. By serving as a selective barrier to the passage of molecules, the plasma membrane determines the composition of the cytoplasm. This ultimately defines the very identity of the cell, so the plasma membrane is one of the most fundamental structures of cellular evolution. The plasma membranes of present-day cells are composed of both

lipids and proteins. The basic structure of the plasma membrane is the phospholipid bilayer, which is impermeable to most water-soluble molecules. The passage of ions and most biological molecules across the plasma membrane is therefore mediated by proteins, which are responsible for the selective traffic of molecules into and out of the cell. Other proteins of the plasma membrane control the interactions between cells of multicellular organisms and serve as sensors through which the cell receives signals from its environment. The plasma membrane thus plays a dual role: It both isolates the cytoplasm and mediates interactions between the cell and its environment.

2.2. WATER RADIOLYSIS AND GENERATION OF REACTIVE OXYGEN SPECIES

In interactions of radiation with water, short lived yet extremely reactive free radicals are produced. The free radicals are highly reactive molecules because they have an unpaired valence electron, consequently can break the chemical bonds and produce chemical changes that lead to biological damage.

Typically, the radiolytic events occur in three main stages taking place on different typical time scales. During the first or “physical” stage, the energy deposition is caused, as described previously, by the incident radiation and secondary electrons are generated. This leads to the formation of ionized water molecules (H_2O^+), excited water molecules (H_2O^*) and sub-excitations electrons (e^-). These resulting species are extremely unstable and undergo fast reorganization in the second or “physicochemical” stage. These processes produce radical and molecular products of radiolysis, occur for example:



and an array of biomolecule-derived carbon-, oxygen-, sulfur-, and nitrogen-centered radicals (i.e., RC^* , RO^* , RS^* , and RN^*) that can in turn lead to the formation of organic peroxides and superoxide anion radicals ($O_2^{\cdot-}$) in the presence of molecular oxygen.

Finally, in a physiologic system, there follows a “biological” stage in which the cells respond to the damage resulting from the products formed in the preceding stages. During this stage the biological responses affecting the long-term consequences of radiation exposure are induced.

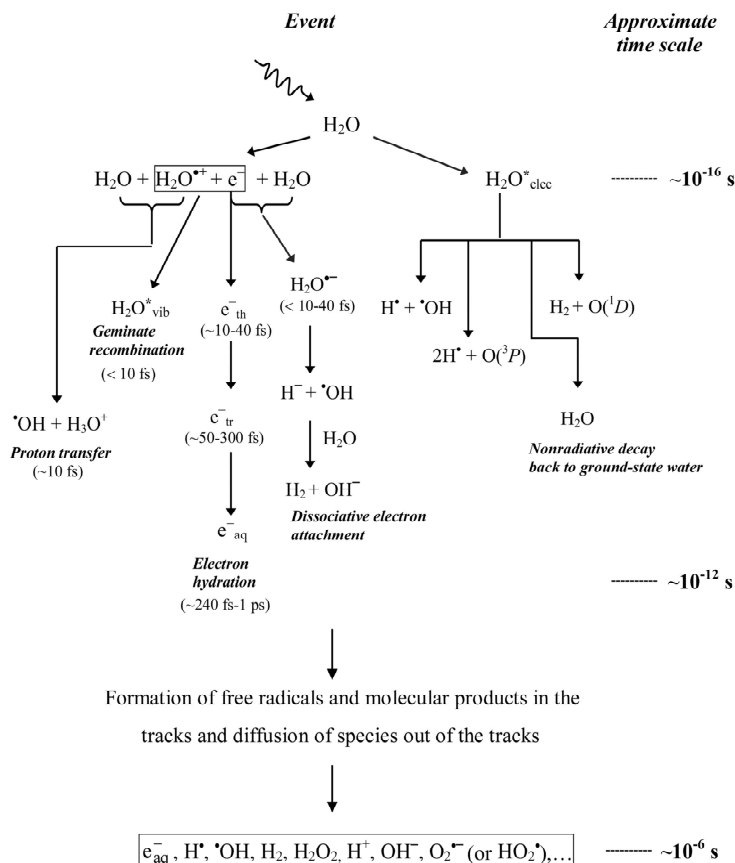


Figure 1.1 Time scale of events in the radiolysis of water by low linear energy transfer radiations

2.3. FUNDAMENTALS OF IONIZING RADIATION BIOCHEMISTRY

- Interaction of IR and IR Effectors with Nucleic Acids**

DNA damaging events inflicted by IR alone include the deleterious alteration of bases and sugars, cross-link formation, single- and double-strand breaks (SSBs/DSBs), and DNA clustering. Of the water radiolysis products, $\text{OH}\cdot$ is the most abundant and particularly destructive to nucleic acid molecules. Radiation damage to deoxyriboses is the primary event underlying strand breakages, which occur in a high frequency and randomly along the DNA backbone in response to both direct $\text{OH}\cdot$ attack and the activity of nucleic acid-binding enzymes. DSBs, in particular, originate through the coordinated reactivity of two $\text{OH}\cdot$ radicals at nearby ribose sites, ultimately leading to strand breaks through subsequent radical pathways.

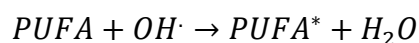
Radiation-induced nucleobase lesions include oxidatively modified bases as well as abasic sites, but do not immediately result in strand breakage. Both $\text{OH}\cdot$ and e^- react with the nucleobases at diffusion-controlled rates, adding to unsaturated bonds and abstracting H from methyl and amino

substituents. These radical products are structurally diverse and are involved in many secondary reactions as oxidants or reductants, depending on the structure and the reactive species in proximity. The immediate response to IR-induced ROS/RNS-mediated DNA damage is the activation of the cell cycle checkpoint response, an intricately controlled network involving sensor, transducer, and effector proteins that respond to the DNA damage signal by initiating a cytoprotective response—the DNA damage response (DDR).

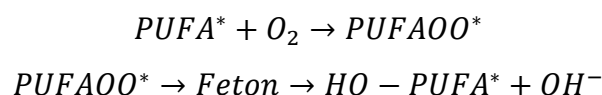
- **Interaction of IR and IR Effectors with Lipids**

Another biomolecule target of radiation-generated ROS is the lipid layer within cell membranes. The lipid component of cell membranes is generally estimated to be ~5 nm in thickness with significant exposure to the aqueous cellular environment. Though radiation is capable of directly damaging lipids, lipid bilayer mimetics have indicated that indirect damage induced by water radiolysis products is a larger contributor toward overall lipid modification by IR. Radiation induces lipid peroxidation leading to an increase in membrane permeability, disruption of ion gradients and other transmembrane processes, and altered activity of membrane-associated proteins.

Polyunsaturated fatty acids are susceptible to free radical attack. The peroxidation was dose- and oxygen-dependent and the extent of peroxidation was inversely proportional to the dose-rate. Lipid peroxidation reactions take place in three steps. The first step is initiation, which produces a fatty acid radical. In polyunsaturated fatty acids, methylene groups next to carbon-carbon double bonds possess especially reactive hydrogen atoms. Lipid peroxidation is most commonly initiated when reactive oxygen species (ROS) such as $\text{OH}\cdot$ and HO_2 interact with a reactive methylene hydrogen atom to produce water and a fatty acid radical:



The second step is propagation. Molecular oxygen reacts with the unstable lipid radical to produce a lipid peroxy radical. This radical is also unstable; it reacts readily with an unsaturated fatty acid to regenerate a new fatty acid radical as well as a lipid peroxide. The generation of the new fatty acid radical in this step reinitiates the cycle. For this reason, this series of reactions is referred to as a lipid peroxidation chain reaction.



The third step is termination. As the chain reaction continues, an increasing concentration of lipid radicals are produced, thereby increasing the probability two lipid radicals will react with each other, which can produce a non-radical species. This constitutes a chain-breaking step, which in combination with the activity of natural radical scavenging molecules in cellular systems ultimately quells the chain reaction.

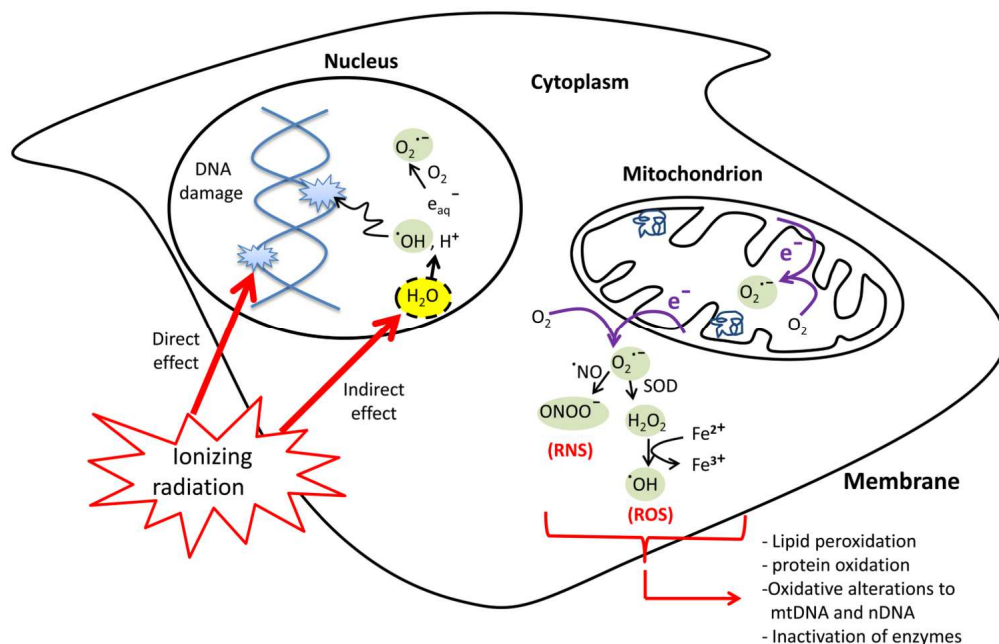


Figure 2.2 The direct and indirect cellular effects of ionizing radiation on macromolecules. Absorption of ionizing radiation by living cells directly disrupts atomic structures, producing chemical and biological changes and indirectly through radiolysis of cellular water and generation of reactive chemical species by stimulation of oxidases and nitric oxide synthases. Ionizing radiation may also disrupt mitochondrial functions significantly contributing to persistent alterations in lipids, proteins, nuclear DNA (nDNA) and mitochondrial DNA (mtDNA).

2.4. IR-INDUCED CELL DEATH OUTCOMES

If the DNA damage can be repaired completely, the cell will continue its cell cycle. In contrast, the consequence of improper DNA repair after irradiation is the onset of cell death, either by apoptosis, mitotic catastrophe or senescence. How the cell will die might be influenced by several parameters: primarily the cell type, the supply with oxygen, the cell cycle phase in which irradiation occurs and, very importantly, the dose and radiation quality, such as dose rate. Hematopoietic and lymphoid cells, and also leukemia cells, are particularly prone to rapid radiation-induced cell death by the apoptotic pathway. In most solid tumors, mitotic cell death (mitotic catastrophe) is as least as

important as apoptosis, and in some cases, it is the only mode of cell death. In contrast, senescence is the fate of irradiated cells in the majority of normal tissues.

- **Apoptosis**

Radiation induces mostly the intrinsic apoptotic pathway (mitochondrial release of cytochrome c and subsequent apoptosome formation), but depending on dose and cell type, the extrinsic apoptotic pathway (death receptor-mediated caspase activation) or the membrane stress pathway (ceramide production and subsequent second messenger signaling) might be the consequence of irradiation.

The intrinsic apoptotic pathway is initiated by signaling following SSBs and DSBs if DNA repair is not successful. The stronger and longer the activation of p53 as a key determinant in DDR, the higher the chances for apoptosis instead of growth arrest. p53 can contribute to both the intrinsic mitochondria-mediated and the extrinsic death-receptor-mediated apoptosis.

- a. The Intrinsic Apoptotic Pathway
- b. The Extrinsic Apoptotic Pathway
- c. The Membrane Stress Apoptotic Pathway

- **Mitotic Catastrophe**

Mitotic catastrophe or mitotic cell death occurs during aberrant mitosis as a result of aberrant chromosome segregation, leading to formation of giant cells with an aberrant spindle, de-condensed chromatin, and multiple micronuclei. This type of cell death is accompanied by the presence of one or more micronuclei and centrosome overduplication. Together with apoptosis, mitotic catastrophe accounts for the majority of IR-induced cancer cell death. Mitotic catastrophe occurs due to faulty mitosis and causes delayed mitotic-linked cell death that takes place via apoptosis or necrosis.

- **Senescence**

Senescent cells are viable but non-dividing and undergo irreversible cell cycle arrest, stop DNA synthesis, and become enlarged and flattened with increased granularity. Cellular senescence is a process that results from multiple mechanisms, including telomere shortening, tumor suppressor signals, and DNA damage. These mechanisms prevent uncontrolled proliferation, and so the cellular senescence can protect cells from developing cancer.

Given that IR-induced senescence can usually be achieved at much lower doses of IR than those required to induce apoptosis and that the reduced dose of IR can help prevent adverse side effects of cancer therapy, other strategies using low-dose IR for cancer therapy deserve much consideration.

Stress-induced premature senescence (SIPS) may greatly affect the efficacy of radiotherapy, and the radiation doses achievable using clinical therapeutic regimens can induce SIPS in specific human tumor cell lines. Irradiated cells undergoing SIPS share many cellular and molecular phenomena with cells undergoing replicative senescence. Although replicative senescence is programmed at times when telomeric DNA ends are exposed, SIPS is not programmed but is instead a response to a given stress. Due to the constitutive activation of telomerase, telomeres are typically stable and replicative senescence is not usually induced in cancer cells. However, many anticancer agents, including IR, can induce SIPS in cancer cells while not affecting telomere lengths. These agents produce double-strand breaks (DSBs), and a common cause of SIPS induction in cancer cells appears to be irreparable DNA breaks.

- **Autophagy**

Cells undergoing autophagy, a form of type II programmed cell death, utilize the autophagic/lysosomal compartment to auto-digest proteins and damaged organelles and to recycle amino and fatty acids. Autophagy is characterized by sequestration of targeted cytoplasmic components and organelles from the rest of the cell within a double-membrane vesicle called the autophagosome. Hyperactivation of the autophagy pathway contributes to cell death but controlled expression has a pro-survival effect.

Autophagy is a genetically regulated stress response seen in some human cancer cell lines exposed to IR. Compared to apoptosis, autophagic cellular changes are observed after IR in any cell line. Similar to the continuing debate as to whether the induction of autophagy results in cancer suppression or progression, the autophagic response of cancer cells to IR reveals somewhat different effects in terms of radiotherapy. IR treatment induces autophagy in both normal and cancer cells.

Some studies suggest that the induction of autophagy might be an advantageous strategy to increase the anticancer effects of radiotherapy and that chemoagent-induced autophagy provokes sensitization of cells to irradiation and increases the anticancer effects of radiotherapy.

3. X RAY IN RADIOTHERAPY

Clinical X ray beams typically range in energy between 10 kVp and 50 MV and are produced when electrons with kinetic energies between 10 keV and 50 MeV are decelerated in special metallic targets.

Most of the electron's kinetic energy is transformed in the target into heat, and a small fraction of the energy is emitted in the form of X ray photons, which are divided into two groups: characteristic X rays and bremsstrahlung X rays.

X rays are used in diagnostic radiology for diagnosis of disease and in radiation oncology (radiotherapy) for treatment of disease. X rays produced by electrons with kinetic energies between:

- between 10 keV and 100 keV are called superficial X rays;
- between 100 keV and 500 keV are called orthovoltage X rays;
- above 1 MeV are called megavoltage X rays.

Orthovoltage ("superficial") X-rays are used in external beam radiotherapy for treating skin cancer and superficial structures. Megavoltage ("deep") X-rays are used to treat deep-seated tumours (e.g. bladder, bowel, prostate, lung, or brain). It is carried out with three types of treatment machine: X ray units, isotope teletherapy units (mainly ^{60}Co units) and linacs. IORT can also be delivered using orthovoltage (250-300 kV) x-rays (X-ray IORT) or low energy (50 kV) x-rays (low-energy IORT).

Typically superficial and orthovoltage X rays are produced with X ray tubes (machines), megavoltage X rays are most commonly produced with linacs and sometimes with betatrons and microtrons. While in this work we will also use orthovoltage X rays produced with Plasma Focus device, which is distinguished by a ultra-high dose rate.

3.1. X-RAY TUBE

Superficial and orthovoltage X rays used in radiotherapy are produced with X ray machines. The main components of a radiotherapeutic X ray machine are: an X ray tube; a ceiling or floor mount for the X ray tube; a target cooling system; a control console; and an X ray power generator.

The electrons producing the X ray beams in the X ray tube (Coolidge tube) originate in the heated filament (cathode) and are accelerated in a vacuum towards the target (anode) by an essentially constant potential electrostatic field supplied by the X ray generator.

The efficiency for X ray production in the superficial and orthovoltage energy range is of the order of 1% or less. Most of the electron kinetic energy deposited in the X ray target (~99%) is transformed into heat and must be dissipated through an efficient target cooling system.

To maximize the X ray yield in the superficial and orthovoltage energy range the target material should have a high atomic number Z and a high melting point.

With X ray tubes, the patient dose is delivered using a timer and the treatment time must incorporate the shutter correction time, which accounts for the time required for the power supply components to attain the steady state operating conditions.

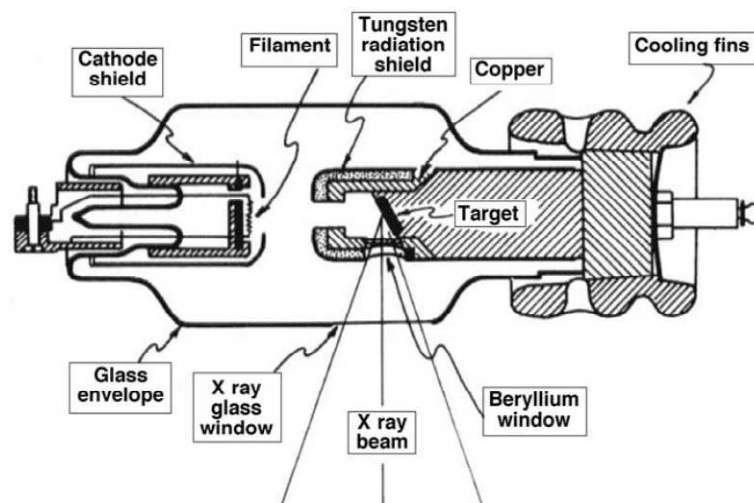


Figure 3.1: Typical therapy X ray tube.

3.1.1. RAY TUBE X BALTEAU CSC320 / 70

The cell samples, sown on the door-samples, were irradiated with the X-ray tube BALTEAU CSC320 / 70 kindly provided by Comecer S.P.A. and the use of which we thank Dr. Stefano Zanella, Head of Calibration Centre (Calibration Centre - COMECER SIT n.065 / r, Castel Bolognese).

3.2. PLASMA FOCUS

The Plasma Focus is a device designed to generate a plasma sheet between two coaxial electrodes by means of a high voltage difference. The energy of a capacitor bank (between a few and a few tens of kilojoule) is instantly transferred to the electrodes producing a plasma sheet which is then pushed toward the open end of the electrodes by $\vec{j} \times \vec{B}$ force. The sheet implodes into a very dense

magnetized plasma pinch. The pinched plasma may reach temperatures of several tens of keV and thermo-nuclear reactions may take place and charged particles be emitted.

The charged particles emission has two main components: an ion beam peaked forward and an electron beam directed backward. For this project, it was thought to use the electron beam to produce x-rays by interaction with appropriate targets (through bremsstrahlung and characteristic emission) for medical applications.

3.2.1.PFMA-3

The Plasma Focus device is provided by DIENCA (Department of Industrial Engineering, University of Bologna, Bologna, Italy) and the use of which we thank Dr. Mario Sumini. This device is named PFMA-3, is of the Mather type. A Mather type Plasma Focus is made of two cylindrical electrodes, closed at one end and open at the other. An insulating sleeve is placed around the base of the inner electrode. These electrodes are connected at the closed end, through a high-speed, high-current switch (usually of a spark gap type), to a capacitor bank where energy is stored. The electrodes are contained in a vacuum chamber filled with a few Torr of a gas, chosen according to the purpose intended. For example: Hydrogen, Deuterium, Tritium, Argon, Neon, other pure gases and gas mixtures have been used [2, 3].

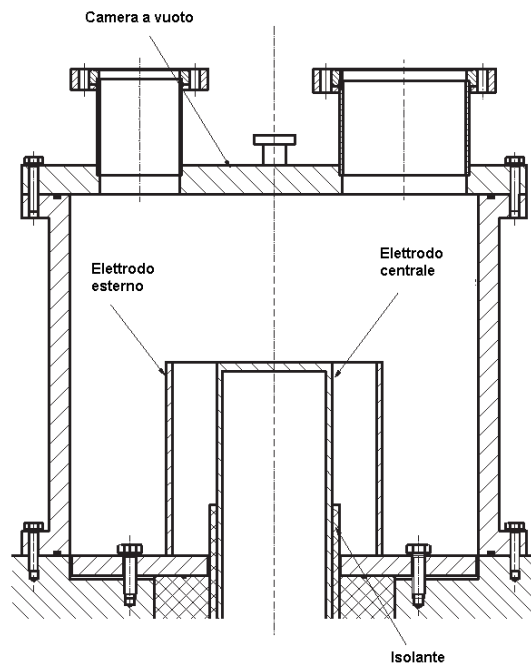


Figure 3.2: Diagram of the Plasma Focus device type Mather.



Figure 3.3: PFMA-3 working room of

3.3. DOSE RATE

IR is effective for the treatment of many cancer types; however, in some patients a few tumors become resistant to radiation, making radiotherapy less effective. Resistance to radiation therapy remains a major clinical problem, leading to a poor outcome for cancer patients. Factors that make cells less radiosensitive are several, as well as removal of oxygen to create a hypoxic state, the addition of chemical radical scavengers, cells synchronized in the late S phase of the cell cycle and the use of low dose rates or multifractionated irradiation. Regarding the latter factor, it is known that for the same dose of radiation, the radiation delivered at a lower dose may produce less killing than radiation delivered at a higher dose rate, because sublethal damage repair occurs during the protracted exposure.

The typical dose rates used in radiotherapy are of the order of:

- 1 Gy/min in standard radiotherapy and high dose rate (HDR) brachytherapy;
- 0.1 Gy/min in TBI;
- 0.01 Gy/min in low dose rate (LDR) brachytherapy.

Many studies have been done on the effects of dose rate brachytherapy, while the effects for external beam are still not widely known. In the Table 3.1 are reported the results obtained in the last three years.

reference	device type	cell type	dose rate		total dose	analyses type	result
			LDR	HDR			
Anne-Sophie Wozny, Gersende Alphonse (2016)	X-RAD 320, PXI (at 250-kV)	The radiosensitive SCC61 and the radioresistant SQ20B cell lines	0.5, 2, or 10 Gy/min		1; 2; 3; 4 e 5 Gy	Analysis of Clonogenic Cell Survival	In response to photon irradiation, a significant change in the survival fraction at 2 Gy (SF2) and the dose for 10% survival (D10) was observed for both cell lines depending on the dose rate.
					1 e 2 Gy	Immunocytochemistry – γ H2AX Assay	For both cell lines irradiated with 2 Gy photons, a higher percentage of residual γ H2AX fluorescence was found at a dose rate of 10 Gy/min compared to the dose rate decreases to 2 Gy/min.
Sreeja Sarojini, Andrew Pecora, et al. (2015)	10X flattening filter-free (FFF) 10 MV X-rays	Melanoma cell lines (WC00046, WC00060, and WC00081)	400 MU/min	2400 MU/min	0.25; 0.50; 0.75; 1; 2 and 8 Gy	MTT assay	A dose rate of 2400MU/min induced an average of 10-fold more apoptosis compared with the control and three-fold more apoptosis compared with the 400 MU/min dose rate.
						DNA-damage assays	The dose rate 2400MU/min caused seven-fold more DNA damage than in nonirradiated controls and nearly two-fold more DNA damage than a 400MU/min dose rate.
						MitoTracker	Semiquantitative analysis of the relative fluorescent intensity showed a 1.3-fold increase in cells treated at 400MU/min and a 2.3-fold increase in cells treated at 2400MU/min compared with controls, indicating that the increase in fluorescence was directly associated with the radiation dose rate
						colony counting	The colony formation assay indicated that cell killing efficiency following irradiation was three-fold greater for WC00046 cells, seven-fold greater for WC00060 cells, and two-fold greater for WC00081 cells at 2400 MU/min compared with 400 MU/min
Shanaz A. Ghandhi, Lubomir B. Smilenov, et al (2015)	Xrad 320 Biological Irradiator (Precision XRay, North Branford CT)	blood from healthy volunteers (5 females and 3 males) between the ages of 26 and 59 years	3.1 mGy/min	1.03 Gy/min	0.56; 2.23; 4.45 Gy	colony counting	We found the broadest changes and highest number of genes affected at 4.45 Gy by both doserates (354 genes changed after LDR 4.45 Gy exposure and 565 genes changed after acute 4.45 Gy exposures at 24 h).
Orlin Gemishev, Stanislav Zapryanov, et al. (2014)	Plasma Focus devices, mather type	The mutant strain Trichoderma reeseiM7		in the order of tens of mSv/ μ s	5–11,000 mSv (thermoluminescent dosimeters (TLD))		In the dose range of 200–1200 mSv, some enhancement of endoglucanase activity was obtained: around 18%–32%, despite the drop of the biomass amount, compared with the untreated material.

Table 3.1: Effects of x-rays at different dose rate (obtained in the last three years).

2. MATERIALS AND METHODS

1. CELLS AND CELL CULTURE

The human metastatic melanoma cell lines SK-MEL-28 were used. Melanomas are, from the point of view radiobiological, the most typical example of radio-resistance, even if the melanoma cells possess an intrinsic radiosensitivity rather variable and closely related to the ability to repair the damage.

Cell were cultured in an incubator at 37 ° C with a humidified atmosphere with 5% CO₂, which is located within the laboratory of the faculty. The culture medium consists of Eangle (E-MEM), to which is added 10% of fetal bovine serum (FBS), 1% L-glutamine, 10% sodium pyruvate and antibiotics: 1% of penicillin and 1% streptomycin.

2. IRRADIATION

Different experiments were designed in three separate groups control cells, irradiated cells at 2 Gy, and irradiated cells at 4 Gy, each group containing subgroups receiving different doses rate: ultra-high dose rate by using a X-ray of PF device and standard dose rate by conventional x-ray tube.

Before the irradiation the cell are seed, 0.1×10^6 for sample, in suitable door samples to allow the beam to reach the sample without interference. Each port samples consists of two discs of mylar thickness of 50 pm, 2 silicone gasket, 2 rings and 1 steel cylinder. The sterilization procedure requires that: initially rinsed in PBS and the mylar is buffered with paper impregnated with alcohol 70% the steel parts and the seals, after which all the components are brought under a hood where they are prepared to be placed in an autoclave at 1200 rpm for 5 min.



Figure 3.1: Sample holder. Left: The individual components of the sample holder: aluminum cylinder, O-rings, discs and rings mylar. Right: The door-assembled sample.

2.1.1. IRRADIATION WITH PF

The radiation is produced by the collision of the back-emitted electrons on a brass disk, with a thickness of 50 microns. The capacitors are set at a potential of 18 kV; the working gas pressure (nitrogen) at the 0.38 to 0.40 mbar value, with pinch current to the peak value 240 kA. The radiation is produced by few pulses spaced from each other by ~30 sec with the duration of the order of the dozens nanosecond for final dose 2 Gy or 4 Gy. One of the door-prepared sample is not irradiated, as it will be used as a control.

The films used to measure the dose erogated by the PFMA3 are the HDV2 and the EBT3. They are placed above the target in a 5 pieces stack formed by a one HDV2, it is used as an electron screen due to the fact that some electrons can escape the target, and four EBT3 films. The first two EBT3 are used in order to films the softer component of the X-ray spectrum generated by the PFMA-3. The EBT3 films are dosimeter used to measure the X-ray dose deposition, they are tissue equivalent dosimeter, and they are read with a CCD scanners.

2.1.2. IRRADIATION WITH RAY TUBE X BALTEAU CSC320/70

The radiation is produced in a conventional manner. To obtain a final dose of 0.5 Gy in the output beam was produced by a V of 60 kV and from an I of 25 mA. The radiation is produced by almost continuous shots with the duration of few sec. The sample holder was positioned at a distance of 40 cm from the heat of the tube, including 1.5 mm aluminum filter placed in front of the beam exit window. Also in this case one of the door-prepared sample is not irradiated, as it will be used as a control. To search the dose received by the cells is the average energy of the radiation per unit mass was calculated knowing the charge discharging.

3. ADHESION AND PROLIFERATION ASSAY

After irradiation of SK-MEL-28 cells, they were detached from the mylar film using trypsin-EDTA (0.02%) and suspended 1:3 in supplemented E-MEM at room temperature. In order to plate the same number of cells for each well, a cell counting by the hemocytometer was performed. Adhesion and proliferation properties were tested on a polystyrene biological multiwell plate (24 wells)

(CELLSTAR, Greiner bio-one). Cells were seeded in a density of $0.015 \times 10^6 \text{ cm}^{-2}$, with 1 ml of culture medium.

We studied cell adhesion and proliferation keeping cells in a CO₂ incubation system integrated within a motorized stage, able to perform time-lapse imaging acquisition even for tens of hours, while for migration test we keep the cells in incubator for 24 h before fluorescence acquisition. In particular, for adhesion experiments cells were allowed to adhere for 2 hours before the acquisition of microscopy images, which were acquired in phase-contrast at 100× of magnification, by the inverse automated optical microscopy Nikon Eclipse-Ti (Nikon, Italy). The same setup was used also for proliferation but in this case, acquisition was performed up to 96 h (four days), every 24 h. The number of adherent and not-adherent cells was determined by classifying them according to morphological parameters such as shape (spherical or non-spherical), structural polarization, the presence of lamellar cytoplasm, leading lamella, and clear signs of stress fibers due to the focal adhesion process. The adhesion rate was defined as the number of adherent cells counted in a focal field of 0.68 mm^2 divided by the total number of cells.

Proliferation analysis was performed counting all cells present in an image field using ImageJ software. The proliferation curves of cell populations have been obtained by counting the number of adherent cells after 24, 48, 72 and 96 h (i.e. until the cell population reached the confluency). The mean number of cells counted in three fixed focal fields sizing 0.68 mm^2 acquired from four wells at each time point was normalized with respect to the number of cells at 24 h from seeding.

The results of the independent experiments were reported as mean \pm SEM. Student's t test was used to compute the probability values (p) in two-group comparison, a minimum threshold of 0.05 was considered for statistical significance.

4. MIGRATION ASSAY

Also for migration assay, after irradiation of SK-MEL-28 cells, they were detached from the mylar film using trypsin-EDTA (0.02%) and suspended 1:3 in supplemented E-MEM at room temperature. In order to plate the same number of cells for each well, a cell counting by the hemocytometer was performed. While for migration test the cells were aliquoted in order to have 50000 cells/well, centrifuged at 1200 RPM for 5 minutes and finally suspended in 100 μl of E-MEM serum free for each well. For this experiment was used a specific multiwell with a porous membrane inside the well, with a pore diameter with size of 8 μm . This insert separates the well volume into two parts: top and bottom compartment. In the bottom was placed supplemented E-MEM (500 μl for well), while in the other one were seeded the cells (serum free condition).

Migration analysis was performed after loading with DAPI (hoechst 33342); for this step culture medium was substituted with E-MEM serum free plus DAPI (1:1000) and leave in incubator for 30 min before washing with PBS. Immediately after the images in Bright Field and DAPI were acquired at 10× of magnification and cells were counted using Nis-Elements software. To count the cells in the bottom compartment allows quantification of migration induced.

The results of the independent experiments were reported as mean \pm SEM. Student's t test was used to compute the probability values (p) in two-group comparison, a minimum threshold of 0.05 was considered for statistical significance.

Results

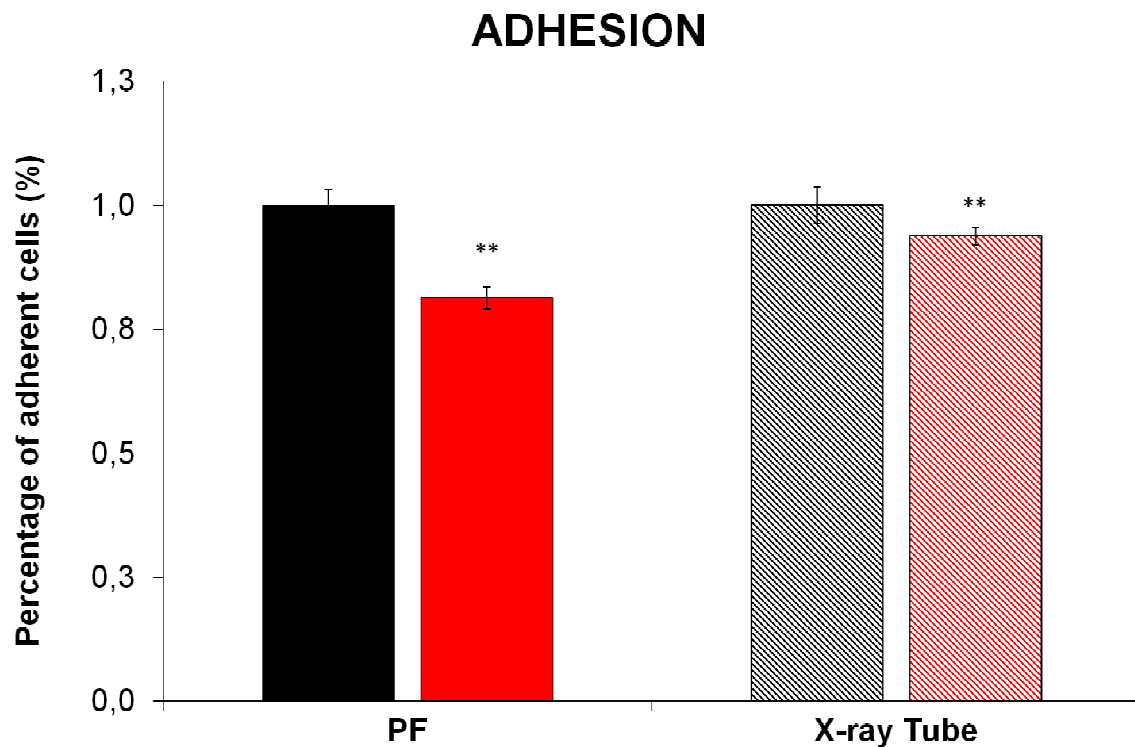


Figure 1: Percentage of adherent cells (SK-MEL-28) irradiated at ultra-high dose rate (with Plasma Focus) and standard dose rate (with x-ray tube) at a total dose of 4 Gy. Irradiated SK-MEL-28 cells, at a total dose of 4 Gy with ultra-high dose rate by Plasma Focus devices (red bar) and standard rate by x-ray tube (red line bar), are compared to non-irradiated cells (control, black bar and black line bar), and between them. The number of adherent cells counted 2 hours after irradiation are divided by the total number of cells and normalized to the corresponding control (%). The rate of proliferation is plotted as the mean \pm S.E.M. of n independent experiments performed in triplicate. P value calculated by student's t-test: ** $p < 0.001$.

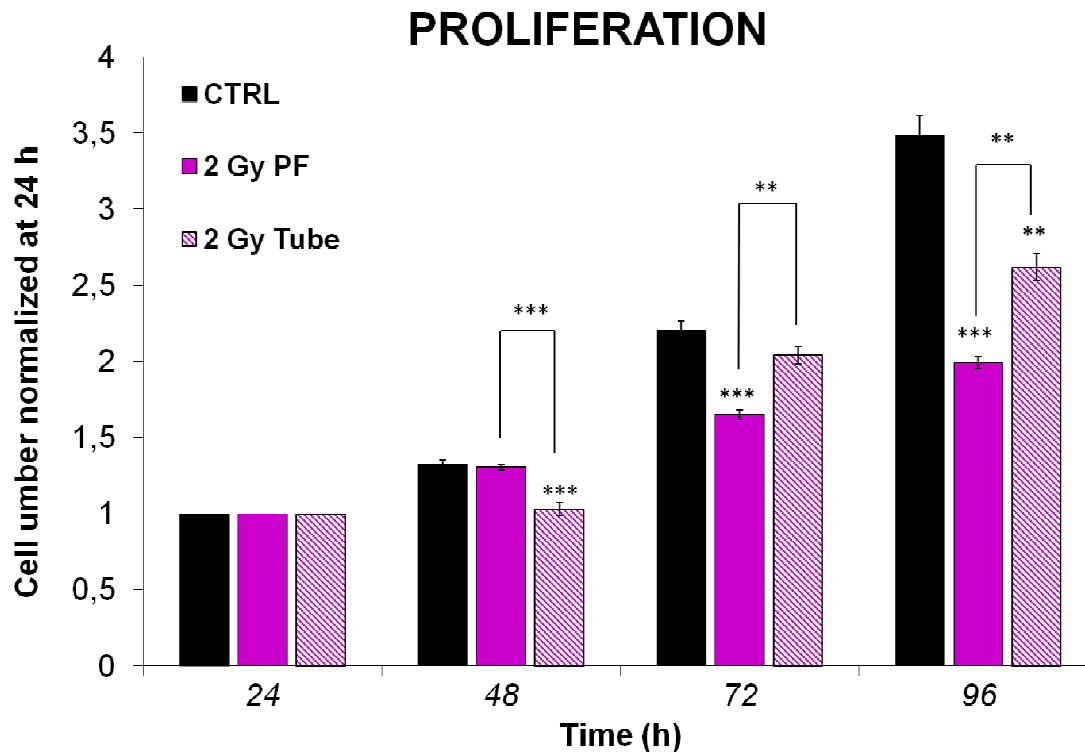


Figure 2: Proliferation rate of SK-MEL-28 cells irradiated at ultra-high dose rate (with Plasma Focus) and standard dose rate (with x-ray tube) at a total dose of 2 Gy. Irradiated SK-MEL-28 cells, at a total dose of 2 Gy with ultra-high dose rate by Plasma Focus devices (red bar) and standard rate by x-ray tube (red line bar), are compared to non-irradiated cells (control, black bar), and between them. The cells were counted at 24, 48, 72 and 96 hours after irradiation and normalized to the corresponding data obtained at 24 hours. The rate of proliferation is plotted as the mean \pm S.E.M. of *n* independent experiments performed in triplicate. P value calculated by student's t-test: **p* < 0.05, ***p* < 0.001, ****p* < 0.0001.

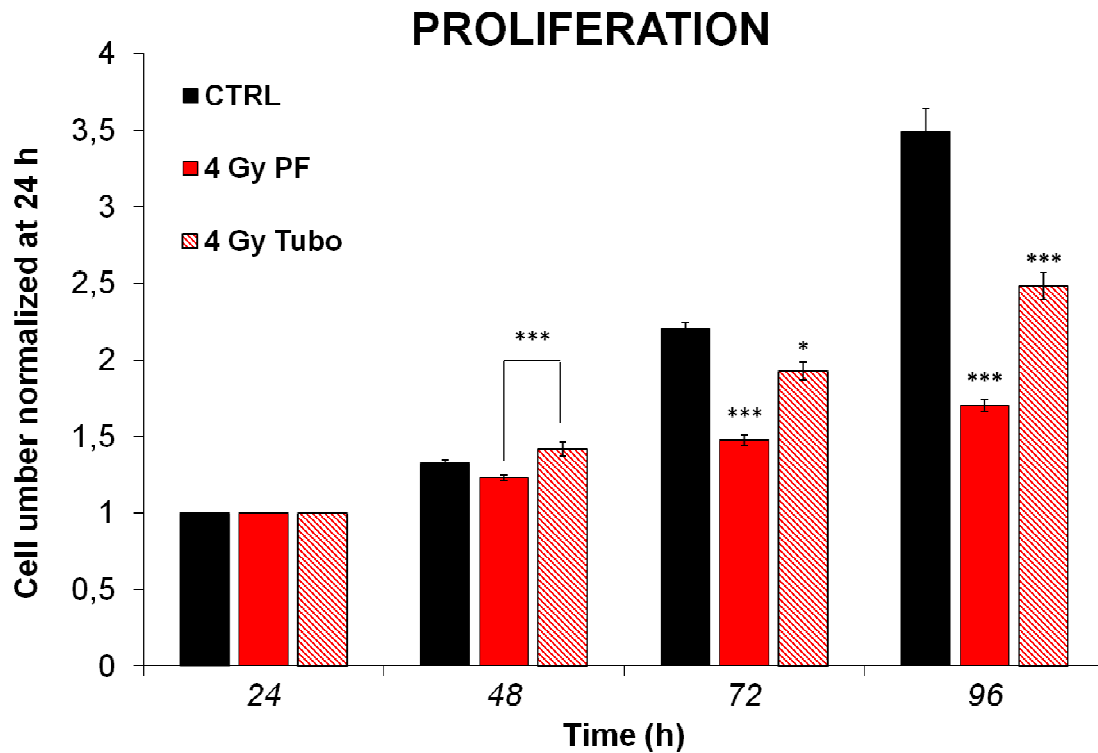


Figure 3: Proliferation rate of SK-MEL-28 cells irradiated at ultra-high dose rate (with Plasma Focus) and standard dose rate (with x-ray tube) at a total dose of 4 Gy. Irradiated SK-MEL-28 cells, at a total dose of 4 Gy with ultra-high dose rate by Plasma Focus devices (red bar) and standard rate by x-ray tube (red line bar), are compared to non-irradiated cells (control, black bar), and between them. The cells were counted at 24, 48, 72 and 96 hours after irradiation and normalized to the corresponding data obtained at 24 hours. The rate of proliferation is plotted as the mean \pm S.E.M. of n independent experiments performed in triplicate. P value calculated by student's t-test: *p < 0.05, **p < 0.001, ***p < 0.0001.

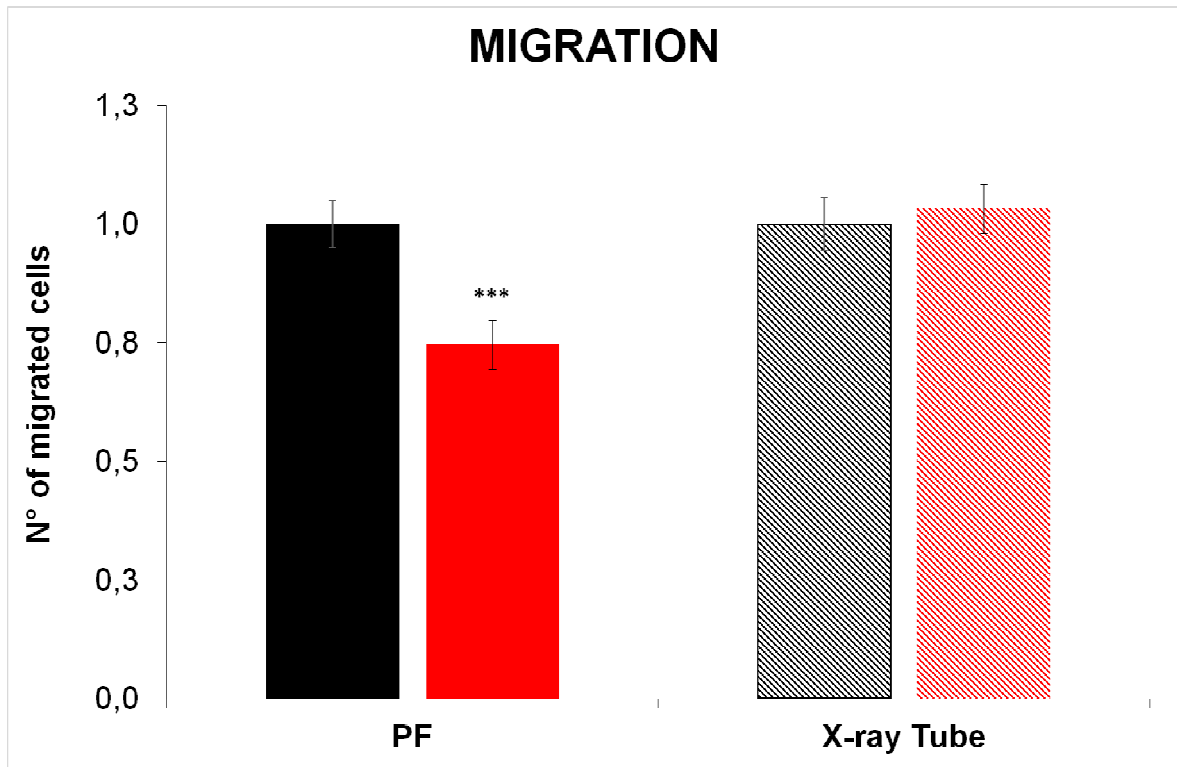


Figure 4: Number of migrated cells (SK-MEL-28) irradiated at ultra-high dose rate (with Plasma Focus) and standard dose rate (with x-ray tube) at a total dose of 4 Gy. Irradiated SK-MEL-28 cells, at a total dose of 4 Gy with ultra-high dose rate by Plasma Focus devices (red bar) and standard rate by x-ray tube (red line bar), are compared to non-irradiated cells (control, black bar and black line bar), and between them. The number of migrated cells, previously treated with DAPI, are counted after 24 hours irradiation and are normalized to corresponding control. The rate of proliferation is plotted as the mean \pm S.E.M. of n independent experiments performed in triplicate. P value calculated by student's t-test: *p < 0.05, **p < 0.001, ***p < 0.0001.

The percentage of cell adherent after 2 hours after the irradiation with ultra-high dose rate and standard dose rate is show in Figure 1. It is observed that the number of adherent cells of the irradiated sample with the ultra-high dose rate is 20% less than the number of adherent cells control, while the sample irradiated with the dose rate standard shows only 8% less compared to the control. The cell proliferation for 96 hours after irradiation with ultra-high dose rate and standard dose rate is show in Figure 2 and Figure 3. At 48 hours after irradiation the proliferation rate, in response to x-ray irradiation induced with ultra-high dose rate, shows a decrease, although not significant, of proliferation for both dose (2 and 4 Gy) compared with control cells. While, for irradiated cells with a standard dose rate was observed a significant decrease of proliferation after 48 hours irradiation at a total dose of 2 Gy but for sample irradiated with total dose 4 Gy was observed a increment of proliferation. Whereas, at 72 hours after the irradiation a significant decrease of proliferation was observed for cells irradiated with ultra-high dose rate for both dose induced. Cells irradiated with standard dose rate show a significant decrease of proliferation only for irradiation to 4 Gy. Finally 96 hours the cells irradiated at both doses induced with either high dose rate both with low dose rate show a significant decrease.

The number of migrated cells 48 hours after the irradiation with ultra-high dose rate and standard dose rate is show in Figure 4. It is observed a significant decrease in migratory capacity only for irradiated cells with an ultra high dose rate, showing 25% less of migrated cells compared to control.

Conclusions

The aim of this study was to compare the effects on the melanoma cell line SK-MEL-28 of x-rays radiations characterized by different dose-rate. Ultra-high and standard dose rate radiation were delivered, respectively, by the PFM-3 plasma focus device and the standard x-ray tube (XRT) at a total dose of 2 or 4 Gy. The results clearly showed that the effects is dose-rate dependent, indeed we observed a greater general decrease of the cellular functionality when ultra-high dose rate were delivered. Furthermore, the data also expressed a dose-dependent trend.

The cellular functionality tests we focused on are mainly targeted to investigate the early effects on the cellular cytoplasmatic district. The postulated increase of reagents species such as radical oxygen or nitrogen species (ROS and NOS) induced by the impact of a photons radiation, can be seen first at the lipidic membrane level and/or on the cytoplasmatic enzymes and proteins. Indeed, we observed a significant decrease of the adhesion capability in both the population of cells irradiated by the two different dose-rate, but in the case of the ultra-high dose rate radiation the impairment induced is more than double. Furthermore, the population of cells irradiated by the ultra-high dose rate showed that the number of migrated cells is significantly lower compared to control. In addition, the comparison with the migratory capability of the population of cells irradiated by the standard dose rate revealed that are significant different. These more efficiency of the ultra-high dose rate on this type of cellular functions might be ascribed at the disruption of the balancing mechanism when the pulses are so close to each other that the chemical reaction with the scavenger molecules is overloaded, impairing the equilibrium.

Going from the cytoplasmatic level to the nucleus, we found that the proliferative capability is more impaired by the ultra-high dose rate irradiation. Following the population growing until 96 hours we observed at 72 hours after irradiations a significant decrease of the number of cells counted, at both doses (2 and 4 Gy) only for the ultra-high dose rate irradiation, while the standard dose rate is not effective at the lower dose. Finally, at 96 hours both data are significant different compare to control, expressing an efficacy of both dose-rate but much more severe in the case of the ultra-high one.

In our opinion, these results are very relevant from a therapeutic point of view since they show that the x-radiation delivered in the ultra-high dose rate way has a greater efficacy in decreasing the ability of melanoma cells to adhere, proliferate and migrate compared to the standard dose rate. The application of the PFM-3 radiation device could improve the effectiveness of radio therapy in the

treatment of superficial and resistant tumors, allowing the use in radio therapy of lower doses than that usually required in conventional treatments.

References

- [A. Virelli, I. Zironi, F. Pasi, E. Ceccolini, R. Nano, A. Facchetti, E. Gavoc, i, M. R. Fiore, F. Rocchi, D. Mostacci, G. Cucchi, G. Castellani, M. Sumini and R. Orecchia (2015)- *Early effects comparison of x rays delivered at high-dose-rate pulses by a plasma focus device and at low dose rate on human tumour cells*]
- [J. C. Edward, D. Chapman, W. A. Cramp And M. B. Yatvin (1984)- *The effects of ionizing radiation on biomembrane structure and function.*]
- [Edouard I. Azzam, Jean-Paul Jay-Gerin, and Debkumar Pain (2012)- *Ionizing radiation-induced metabolic oxidative stress and prolonged cell injury*]
- [Juliann G. Kiang, Risaku Fukumoto and Nikolai V. Gorbunov (2012)- *Lipid Peroxidation After Ionizing Irradiation Leads to Apoptosis and Autophagy*]
- [Julie A. Reisz, Nidhi Bansal, Jiang Qian, Weiling Zhao, and Cristina M. Furdui (2014)- *Effects of Ionizing Radiation on Biological Molecules—Mechanisms of Damage and Emerging Methods of Detection.*]
- [Byeong Mo Kim , Yunkyung Hong, Seunghoon Lee, Pengda Liu, Ji Hong Lim, Yong Heon Lee, Tae Ho Lee, Kyu Tae Chang, and Yonggeun Hong (2015)- *Therapeutic Implications for Overcoming Radiation Resistance in Cancer Therapy.*]
- [2016- *Cellular Pathways in Response to Ionizing Radiation and Their Targetability for Tumor Radiosensitization.* Patrick Maier *, Linda Hartmann, Frederik Wenz and Carsten Herskind]
- [Orlin Gemishev, Stanislav Zapryanov, Alexander Blagoev, Maya Markova, and Valentin Savov (2014)- *Effect of multiple short highly energetic X-ray pulses on the synthesis of endoglucanase by a mutant strain of Trichoderma reesei M7.*]
- [Shanaz A. Ghandhi, Lubomir B. Smilenov, Carl D. Elliston, Mashkura Chowdhury, and Sally A. Amundson (2015)- *Radiation dose rate effects on gene expression for human biodosimetry*]
- [Sreeja Sarojini, et al. (2015)- *A combination of high dose rate (10X FFF/2400 MU/min/10 MV X-rays) and total low dose (0.5 Gy) induces a higher rate of apoptosis in melanoma cells in vitro and superior preservation of normal melanocytes.*]
- [Anne-Sophie Wozny, Gersende Alphonse, Priscillia Battiston-Montagne, Stéphanie Simonet, Delphine Poncet, Etienne Testa, Jean-Baptiste Guy, Chloé Rancoule, Nicolas Magné, Michael Beuve and Claire Rodriguez-Lafrasse (2016)- *Influence of dose rate on the cellular response to low- and high-LET radiations.*]